Journal of Inorganic and General Chemistry
ZAAC
Zeitschrift für anorganische und allgemeine Chemie
www.zaac.wiley-vch.de
RESEARCH ARTICLE
Check for updates
DOI: 10.1002/zaac.202500150

Heterobimetallic Pt(II) Complexes Supported by 1,8-Naphthyridine Ligands Confirm the Rotation of C_6F_5 Groups about the Pt—C Bond

Alberto Pérez-Bitrián,* Carmen Munarriz, Angel J. Rueda, Antonio Martín, and José M. Casas*

Dedicated to the 120th Birthday of Prof. Dr. Christian Limberg and Prof. Dr. Franc Meyer

The ligand 1,8-naphthyridine (napy) exhibits a rich coordination chemistry arising from the disposition of its two nitrogen atoms. In this work, the mononuclear platinum complex *cis*-[Pt(C_6F_5)$_2$(napy)$_2$] was synthesized and used to prepare other platinum complexes such as *cis*-[Pt(C_6F_5)Cl(napy)$_2$]. More importantly, its suitability as precursor for the synthesis of other heterobimetallic donor–acceptor complexes of the type Pt → M (M = Ag, Cu) was explored. This way, complexes *cis*-[Pt(C_6F_5)$_2$(μ-napy)$_2$Ag($OClO_3$)] and *cis*-[Pt(C_6F_5)$_2$(μ-napy)$_2$Cu(NCMe)][PF_6] were prepared, in which two napy ligands bridge both metal atoms. In the rare Pt → Cu donor–acceptor complex, the MeCN ligand was easily substituted by a chlorido ligand, resulting in *cis*-[Pt(C_6F_5)$_2$(μ-napy)$_2$CuCl] and [{Pt(C_6F_5)$_2$(μ-napy)$_2$Cu}$_2$(μ-Cl)][PF_6], depending on the stoichiometry. In all cases, the free rotation of the C_6F_5 ligands about the Pt—C bonds in solution at room temperature can be stopped at low temperature.

1. Introduction

The heterocycle 1,8-naphthyridine (napy) is a unique ligand in coordination chemistry due to the particular disposition of the two nitrogen atoms, which are separated only by a short distance of 2.2 Å.[1,2] This results in the napy ligand offering a variety of coordination modes, namely monodentate, bidentate chelating, and bidentate bridging (**Figure 1**). Nevertheless, the parallel arrangement of the electron pairs of both N-donor atoms makes it a suitable bridging ligand yet complicates the formation of four-membered chelating rings due to their high directionality, not really pointing in the appropriate direction. In fact, it has been proved that ancillary ligands and solvents can influence the preferred coordination mode.[1]

Among the various metal centers that can engage in the formation of complexes with napy ligands, platinum is one of the few that offers examples for all the coordination possibilities (see Figure 1). Monodentate napy can be found in [Pt(C_6F_5)$_3$(napy)]$^-$,[3] as well as in the homoleptic [Pt(napy)$_4$]$^{2+}$.[4] A prototypical example of a platinum complex in which the napy ligand acts as a bridge between two platinum centers is the homoleptic paddlewheel complex [Pt$_2$(napy)$_4$]$^{4+}$.[4] In the case of the prevalent square-planar platinum(II) geometry, having napy as a chelating ligand implies a low directionality of the lone pairs, which can anyway be achieved in [Pt(C_6F_5)$_2$(napy)] when reacting the labile *cis*-[Pt(C_6F_5)$_2$(thf)$_2$] (thf = tetrahydrofuran) with one equivalent of napy.[5] In fact, this is due to the steric encumbrance provided by the pentafluorophenyl ligands, which cannot coexist in a binuclear complex of the form [Pt$_2$(C_6F_5)$_4$(μ-napy)$_2$] that would render the platinum centers to close to each other. Nevertheless, exchanging one of the C_6F_5 ligands by a chlorido one ensures enough space to stabilize a binuclear species of the type [Pt$_2$(C_6F_5)$_2$Cl$_2$(μ-napy)$_2$].[6] For this, a detour must be taken by protonating the napy chelate in the mononuclear precursor with HCl to obtain *cis*-[Pt(C_6F_5)$_2$Cl(napyH)], which upon thermal activation eliminates C_6F_5H, therefore provoking the dimerization through bridging napy ligands. Further examples of homobimetallic platinum(II) complexes with a bridging napy ligand are the family of the binuclear species [Pt$_2$(μ-napy)(μ-X)(C_6F_5)$_4$]$^-$ (X = Cl, Br, I, OH, SPh, C_6F_5).[3]

Among the three coordination modes of the napy ligand, it is the monodentate fashion that opens the door to an even richer chemistry due to the free nitrogen atom that can act as a reaction site. Interestingly, this has been exploited, yet in the case of Ru complexes for preventing the cleavage of Ru—CO bonds upon electrochemical reduction of the precursor, which leads to a nucleophilic attack of the non-bonded N atom to the carbonyl carbon atom of the CO ligand.[7–9] Furthermore, the non-coordinated nitrogen atom can enable the coordination of yet another metal center, as it is the case of the formation of [NBu_4][Pt$_2$(μ-napy)(μ-C_6F_5)(C_6F_5)$_4$] from [NBu_4][Pt(C_6F_5)$_3$(napy)] and *cis*-[Pt(C_6F_5)$_2$(thf)$_2$].[3]

A. Pérez-Bitrián,[+] C. Munarriz, A. J. Rueda, A. Martín, J. M. Casas
Instituto de Síntesis Química y Catálisis Homogénea (iSQCH), CSIC-Universidad de Zaragoza, C/Pedro Cerbuna 12, 50009 Zaragoza, Spain
E-mail: alberto.perez-bitrian@hu-berlin.de; casas@unizar.es
[+]Present address: Institut für Chemie, Humboldt-Universität zu Berlin, Brook-Taylor-Straße 2, 12489 Berlin, Germany

Supporting information for this article is available on the WWW under https://doi.org/10.1002/zaac.202500150

Journal of Inorganic and General Chemistry
ZAAC
Zeitschrift für anorganische und allgemeine Chemie

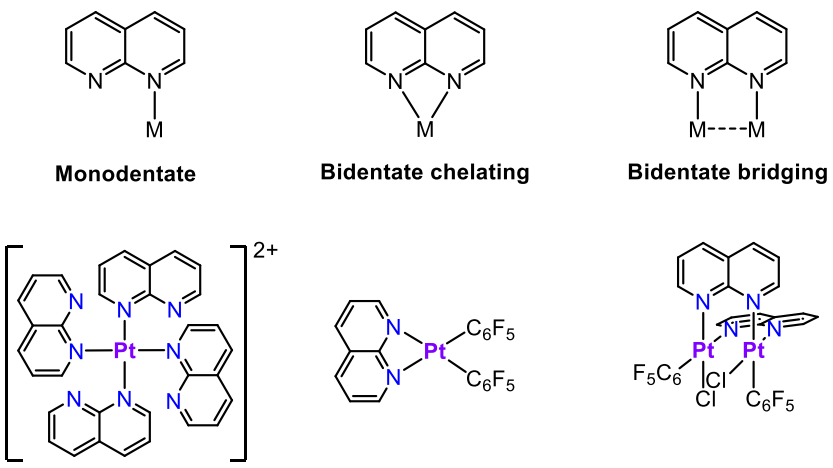

Figure 1. Coordination modes of 1,8-naphthyridine and representative examples of Pt(II) complexes.

Homo and heterobimetallic platinum complexes are well-known for their applications in different fields, ranging from their photophysical properties to their involvement in catalytic transformations.[10–14] Particularly interesting are heterobimetallic complexes containing the so-called dative or donor–acceptor interactions.[12–17] Square-planar Pt(II) centers (d^8) are here popular electron donors, due to the higher-energy occupied d_z^2 orbital pointing in the perpendicular direction of the plane,[18,19] which is therefore in a suitable orientation to establish Pt → M donor–acceptor interactions with Lewis acidic M centers (normally d^{10} or s^2). Among the acidic metal acceptors, group 11 elements are especially popular,[15–17] with Pt—Ag being the most abundant interactions of this kind.[20–26] Fewer examples containing Pt—Au bonds are known,[25–39] and Pt—Cu complexes are even more scarce, yet of increasing interest, especially as models for intermediates in transmetalation processes or in metal−metal cooperative bond activation.[26,33,34,40–42]

Surprisingly, despite the ability of the napy ligand to stabilize binuclear systems, its suitability to engage in heterobimetallic platinum complexes has not been explored so far. In fact, to the best of our knowledge, only the heterobimetallic [PtPd(μ-napy)(μ-OH)$(C_6F_5)_4]^-$ complex has been mentioned in the literature.[3] Within this context, we envisioned the use of 1,8-naphthyridine to form heterobimetallic complexes upon coordination of acidic centers through the second nitrogen of napy ligands already coordinated to a platinum(II) center in a monodentate fashion. In particular, here we report on the synthesis of *cis*-$[Pt(C_6F_5)_2(napy)_2]$ and its use as starting material to prepare binuclear complexes, with a special focus on the stabilization of Pt—Cu species.

2. Results and Discussion

2.1. Synthesis and Characterization of *cis*-$[Pt(C_6F_5)_2(napy)_2]$ (1) and Related Mononuclear Pt(II) Complexes

The $Pt(C_6F_5)_2$ moiety has already been demonstrated to be suitable to stabilize platinum(II) binuclear complexes, something that can be achieved as long as the binucleating ligand gives enough space for the two couples of C_6F_5 to coexist.[6] Due to the small bite angle of the napy ligand, we envisioned that the addition of two equivalents of napy to *cis*-$[Pt(C_6F_5)_2(thf)_2]$ instead of one would lead to the *cis*-$[Pt(C_6F_5)_2(napy)_2]$ (**1**) complex instead of the chelating $[Pt(C_6F_5)_2(napy)]$. In fact, this synthetic route allows to obtain compound **1** in a straightforward way (**Figure 2**a) and *cis*-$[Pt(C_6F_5)_2(napy)_2]$ can be then obtained as a yellow solid with high purity and in high yield (80%). Interestingly, compound **1** can also be prepared with a fewer synthetic cost starting either from $[N^nBu_4]_2[Pt_2(C_6F_5)_4(\mu\text{-}Cl)_2]$ or even from the very first starting material $[N^nBu_4]_2[Pt(C_6F_5)_4]$ (Figure 2a), therefore circumventing the isolation of *cis*-$[Pt(C_6F_5)_2(thf)_2]$. The reaction of $[N^nBu_4]_2[Pt(C_6F_5)_4]$ with 2 equivalents of $HClO_4$ in MeOH in the presence of an excess of napy at room temperature leads to complex **1** in 75% isolated yield upon cleavage of two of the Pt—C bonds. Alternatively, refluxing a mixture of $[N^nBu_4]_2[Pt_2(C_6F_5)_4(\mu\text{-}Cl)_2]$ and excess of napy in $CHCl_3$ for 5 h also results in the formation of **1** with a slightly increased yield of 83%.

The nature of complex **1** was proved by NMR spectroscopy. In the ^{1}H NMR spectrum, six signals corresponding to the napy ligands appear. Only one of them exhibits satellites due to the coupling to the ^{195}Pt NMR-active center, which is assigned to the H in *ortho* position of the ring that is coordinated to the platinum center. This demonstrates the monodentate coordination fashion of the napy ligand in **1**, which is further backed by the presence of six signals due to the two inequivalent fused pyridine rings of the ligand. Also, no dissociation-coordination equilibrium of the napy ligand can be invoked because such a situation might lead to the ^{195}Pt satellites of the most deshielded *ortho*-H signal being not so clearly visible. The ^{19}F NMR spectrum in deuterated acetone shows one set of signals for the C_6F_5 groups, indicating that they are chemically equivalent. In the signal corresponding to the *ortho*-F, the presence of ^{195}Pt satellites evidences the coordination of the aryl moieties to the Pt(II) center, since the $^3J_{F\text{-}Pt} =$ 487 Hz is typical for this oxidation state.[3,5,6,43,44] The fact that only one signal appears for the F in *ortho* position indicates that both C_6F_5 ligands have free rotation about the Pt−C_{ipso} axis, therefore

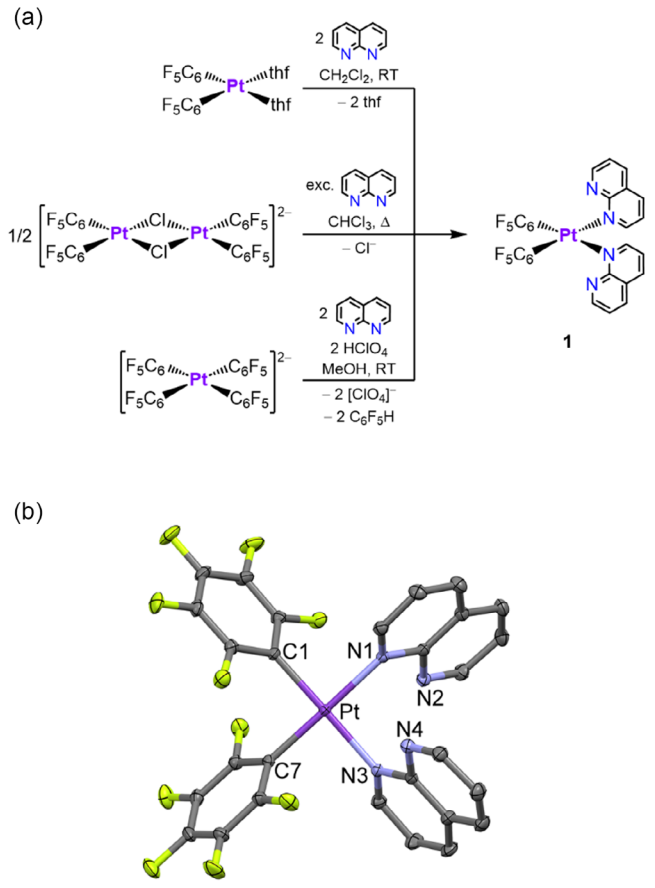

Figure 2. a) Synthetic routes to complex *cis*-[Pt(C_6F_5)$_2$(napy)$_2$] (**1**). In all cases, the cation is [N^{n}Bu$_4$]$^+$. b) Molecular structure of complex *cis*-[Pt(C_6F_5)$_2$(napy)$_2$] (**1**) in the solid state. Hydrogen atoms of napy ligands have been omitted for clarity. Displacement ellipsoids are set at 50% probability. Selected bond lengths [pm] and angles [°]: Pt—N1 209.41(16), Pt—N3 209.25(16), Pt—C1 200.48(18), Pt—C7 200.13(18), N3—Pt—N1 91.48(6), C1—Pt—N1 89.71(7), C7—Pt—C1 89.57(7), C7—Pt—N3 89.32(7), C1—Pt—N3 176.81(7), C7—Pt—N1 178.23(6). For crystallographic details see the Supporting Information.

rendering these two F atoms chemically equivalent in solution. Nevertheless, when the NMR is measured in CD_2Cl_2 at lower temperatures, the signal corresponding to the *ortho*-F splits into two at 183 K, indicating the inequivalence of these two atoms within each ring (see Figure S14, Supporting Information). This is additionally accompanied by a broadening of the resonance of the *meta*-F atoms (see Figure S13, Supporting Information). Moreover, when the measurements are carried out in $(CD_3)_2CO$, the *ortho*-F signals appear clearly resolved as two different resonances already at 208 K (Figure S15, Supporting Information).

The NMR data of **1** could not confirm unequivocally the arrangement of the napy ligands around the Pt(II) center. There are two possibilities that may justify the NMR signals for this couple of ligands in complex **1**: the presence of a plane or a C_2 axis of symmetry. For that, determination of the crystal structure of compound **1** was necessary. Suitable single crystals for X-ray diffraction were obtained by slow diffusion of a layer of *n*-hexane into a solution of complex *cis*-[Pt(C_6F_5)$_2$(napy)$_2$] (**1**) in acetone at 243 K. The determination of the crystal structure of complex **1** enabled to further confirm the monodentate coordination fashion of both napy ligands, already derived from the ^{1}H NMR spectrum. Furthermore, the molecular structure provides a precise proof of the *cis* arrangement of the napy ligands with respect to the platinum coordination plane in the solid state (Figure 2b). Formally, the napy ligands and the pentafluorophenyl groups are related to each other by a C_2 symmetry axis contained in the platinum coordination plane, which in fact, exhibits a slightly distorted square-planar geometry ($\tau_4 = 0.02$).[45] Interestingly, the molecular structure of **1** also indicates that the coordination of the napy ligands takes place with retention of the stereochemistry when using *cis*-[Pt(C_6F_5)$_2$(thf)$_2$] or [N^{n}Bu$_4$]$_2$[Pt$_2$(C_6F_5)$_4$(μ-Cl)$_2$] as starting materials, and it is the same achieved when starting from the homoleptic complex [N^{n}Bu$_4$]$_2$[Pt(C_6F_5)$_4$]. IR data are also in agreement with the *cis* arrangement of both C_6F_5 groups, since the two bands at 808 and 798 cm^{-1} can be assigned to the so-called 'X-sensitive' mode of the C_6F_5 groups and are characteristic of this coordination fashion.[46]

Compound **1** arises as a suitable starting material to form binuclear Pt complexes with bridging napy ligands, due to the freedom of the two nitrogen atoms to coordinate a second metal center. The formation of a [Pt$_2$(C_6F_5)$_4$(μ-napy)$_2$] complex could be potentially achieved by reaction of **1** with one equivalent of *cis*-[Pt(C_6F_5)$_2$(thf)$_2$]. Unfortunately, this reaction failed, resulting instead in the formation of *cis*-[Pt(C_6F_5)$_2$(napy)], which highlights the close proximity that the napy ligand enforces between the two Pt(II) centers, thereby preventing the coexistence of four pentafluorophenyl groups in such a situation due to significant steric encumbrance.[6]

Nevertheless, compound **1** could be used as starting material to prepare *cis*-[Pt(C_6F_5)$_2$Cl(napyH)] (**2**) upon reaction with HCl (0.25 M in MeOH) in $CHCl_3$ (**Figure 3a**). Compound **2**, which is obtained as a yellow solid, was also reported to be prepared by reaction of [Pt(C_6F_5)$_2$(napy)] with HCl in MeOH, taking advantage of the high strain of the four-member chelate that allows easy opening (Figure 3a).[6] Compound **2** is the starting material required to prepare [Pt$_2$(C_6F_5)$_2$Cl$_2$(μ-napy)$_2$] upon reflux in chloroform.[6] Nevertheless, when starting from **1**, one of the napy ligands dissociates from the platinum(II) center as a by-product, which has to be washed from the precipitated solid material with $CHCl_3$ and Et_2O to obtain **2** in pure form before refluxing it in $CHCl_3$ to yield [Pt$_2$(C_6F_5)$_2$Cl$_2$(μ-napy)$_2$]. Alternatively, if the free napy ligand is not separated and the obtained mixture directly refluxed in $CHCl_3$ without further purification, it re-coordinates to the platinum center once the Pt—C bond is protonated (with formation of C_6F_5H), preventing dimerization and leading to the formation of *cis*-[Pt(C_6F_5)Cl(napy)$_2$] (**3**, Figure 3a). Compound **3** is obtained as a pale yellow solid, which can be isolated in 47% yield. The twelve aromatic protons observed in the ^{1}H NMR spectrum account for the two chemically inequivalent napy ligands, indicating a *cis* arrangement with different ligands *trans* to them. One of them shows prominent shoulders due to the coupling to the ^{195}Pt nucleus, whereas in the signal corresponding to the other ligand, these are not so clear. In the ^{19}F NMR spectrum, one set of signals for the pentafluorophenyl ligand is observed, yet the *ortho*-F signal is barely visible. The presence of some type

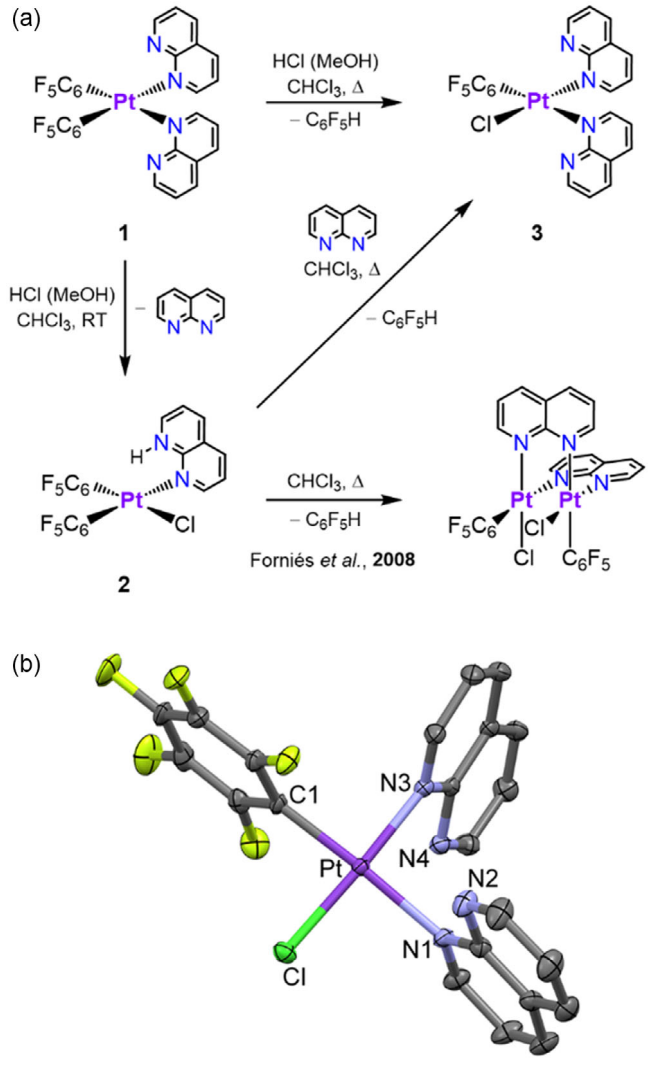

Figure 3. a) Reactivity of *cis*-[Pt(C_6F_5)$_2$(napy)$_2$] (**1**) leading to the formation of mononuclear Pt(II) complexes *cis*-[Pt(C_6F_5)$_2$Cl(napyH)] (**2**) and *cis*-[Pt(C_6F_5)Cl(napy)$_2$] (**3**). b) Molecular structure of complex *cis*-[Pt(C_6F_5)Cl(napy)$_2$] (**3**) in the solid state. Hydrogen atoms of napy ligands have been omitted for clarity. Displacement ellipsoids are set at 50% probability. Selected bond lengths [pm] and angles [°]: Pt—N1 210.6(2), Pt—N3 203.7(2), Pt—C1 199.6(3), Pt—Cl 228.29(6), N3—Pt—N1 93.73(9), C1—Pt—N3 89.02(10), C1—Pt—Cl 88.14(8), N1—Pt—Cl 89.07(6), N3—Pt—Cl 176.98(6), C1—Pt—N1 176.73(10). For crystallographic details see the Supporting Information.

of exchange process arising from the strong *trans* influence of the C_6F_5 ligand[47] might account for both the shape of the *ortho*-F signal and for the lack of ^{195}Pt satellites in one of the *ortho*-H signals of the ring of one napy ligand coordinated to the platinum center. The ν(C—F) absorption at 953 cm^{-1} in the IR spectrum of **3** is in agreement with the oxidation state II of the platinum center, whereas the band at 346 cm^{-1} can be assigned to the ν(Pt—Cl) vibration.

Compound *cis*-[Pt(C_6F_5)Cl(napy)$_2$] (**3**) could be crystallized, and the determination of the molecular structure in the solid state allowed precise confirmation of the *cis* arrangement (and therefore inequivalence) of the napy ligands, both showing a monodentate coordination mode to platinum (Figure 3b). This mononuclear complex shows a square-planar coordination environment at the platinum(II) center ($\tau_4 = 0.04$),[45] yet slightly more distorted than in the case of complex **1**, with each of the non-coordinated nitrogen atoms of the napy ligands located on a different side of the platinum coordination plane (see Figure 3b). Each napy has a different ligand in *trans* position to complete the tetracoordination at the platinum(II) center, one chlorido ligand and one pentafluorophenyl group. The two Pt—N distances are different, allowing us to verify the higher *trans* influence of the C_6F_5 group,[47] which leads to a clearly longer Pt—N bond with the napy *trans* to it (210.6(2) pm), than that *trans* to the chlorido ligand (203.7(2) pm).

2.2. Synthesis and Characterization of Binuclear Complexes with Pt—M Donor–Acceptor Bonds (M = Ag, Cu)

Due to the suitability of platinum(II) to act as a Lewis base and establish Pt → M donor–acceptor bonds, in particular with group 11 metals (see Introduction), we envisioned the use of **1** as a promising scaffold to coordinate such metals, the compounds being further stabilized by bridging napy ligands. As a proof of concept, we started with silver(I), which is well known to engage in such kind of interactions. In this regard, $AgClO_4$ is a suitable precursor, which would provide the perchlorate anion either as the counterion of a cationic complex or as a ligand. In fact, the reaction of **1** with the equimolar amount of $AgClO_4$ in THF in the dark leads to the formation of the binuclear Pt(II)—Ag(I) complex *cis*-[Pt(C_6F_5)$_2$(μ-napy)$_2$Ag($OClO_3$)] (**4**, **Figure 4**a) as a yellow solid in high yield (93%).

The X-ray diffraction study of compound **4** enabled the precise confirmation of the nature of this binuclear complex containing a Pt → Ag donor–acceptor bond supported by two bridging napy ligands, which remain in *cis* disposition, as were also in precursor **1** (see Figure 4b). The five-coordinate platinum center presents a distorted square-pyramidal structure ($\tau_5 = 0.07$),[48] with the silver atom occupying the apical position. For its part, the four-coordinate silver(I) center exhibits a notably distorted tetrahedral structure ($\tau_4 = 0.61$),[45] formed by two nitrogen atoms of the two napy ligands, the platinum atom and one oxygen atom of the perchlorate group. It should be noted that despite [ClO_4]$^-$ being a weakly coordinating anion, it acts as a ligand towards the silver center in the absence of a better ligand to complete the coordination sphere. The weakness of the interaction is reflected by the long Ag—O1 length of 236.5(3) pm. The Pt—Ag axis is almost perpendicular to the basal plane of the square pyramid containing the platinum center, the angle between the Pt—Ag axis and the vector perpendicular to the best coordination plane of the platinum center being 10.8(1)°. The Pt—Ag bond length (279.60(3) pm) is in the usual range found for other related Pt(II) → Ag(I) donor–acceptor complexes,[17] even containing C_6F_5 groups and/or unsupported Pt—Ag interactions.[49–51]

This structure could be further confirmed by spectroscopic investigations. First, the ν(C—F) band of the C_6F_5 groups at 957 cm^{-1} indicates that the Pt(II) stays in oxidation state II, whereas the two X-sensitive bands at 798 and 811 cm^{-1} point towards the presence of two pentafluorophenyl groups in *cis* arrangement. By its side, NMR spectroscopy provides a much more insightful

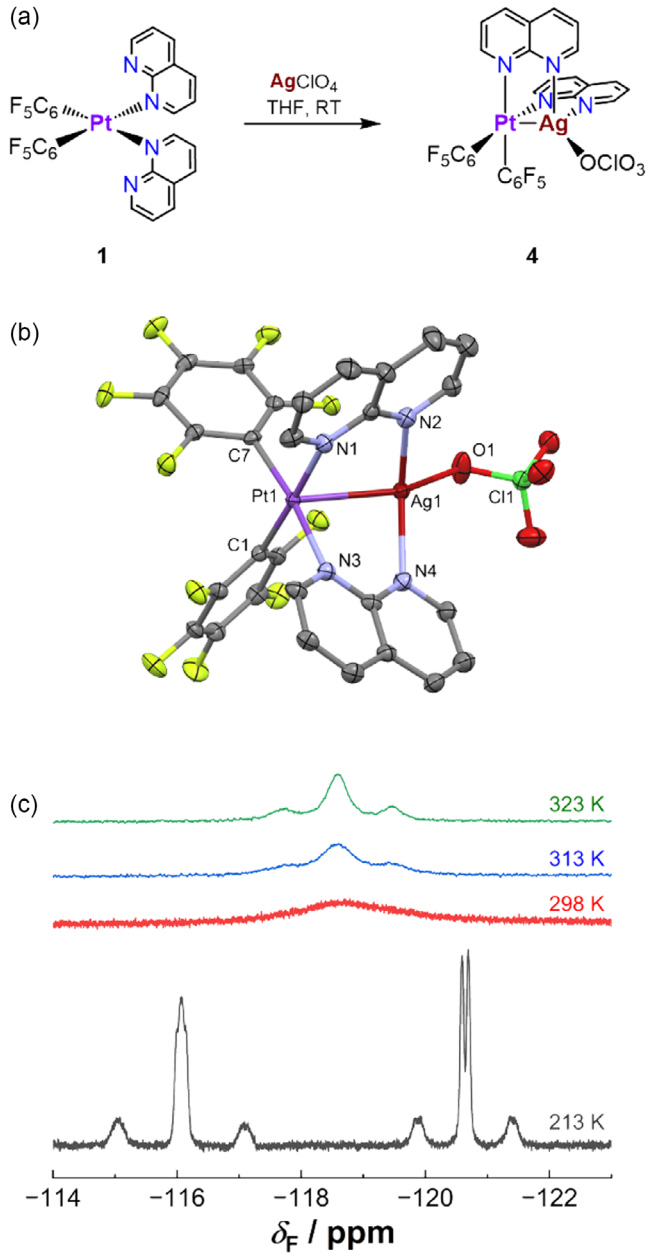

Figure 4. a) Synthesis of the Pt(II)−Ag(I) complex **4**. b) Molecular structure of complex *cis*-[Pt(C_6F_5)$_2$(μ-napy)$_2$Ag($OClO_3$)] (**4**) in the solid state. Hydrogen atoms of napy ligands have been omitted for clarity. Displacement ellipsoids are set at 50% probability. Selected bond lengths [pm] and angles [°]: Pt−Ag 279.60(3), Pt−C1 201.0(3), Pt−C7 202.3(3), Pt−N1 213.5(3), Pt−N3 212.1(3), Ag−N2 225.3(3), Ag−N4 223.2(3), Ag−O1 236.5(3), C1−Pt−Ag 98.42(10), C7−Pt−Ag 101.32(10), N1−Pt−Ag 84.62(7), N3−Pt−Ag 84.25(8), C7−Pt−C1 86.68(13), C1−Pt−N3 87.63(12), C7−Pt−N1 92.64(12), N3−Pt−N1 92.80(11), C1−Pt−N1 176.96(12), C7−Pt−N3 172.56(12), O1−Ag−Pt 150.25(7), N4−Ag−N2 124.37(11), N4−Ag−O1 115.01(11), N2−Ag−O1 105.84(12), N4−Ag−Pt 80.49(7), N2−Ag−Pt 82.10(7). For crystallographic details see the Supporting Information. c) ^{19}F NMR spectra of **4** (377 MHz, $(CD_3)_2CO$) at variable temperatures depicting the signal(s) of the *ortho*-F atoms of the C_6F_5 groups.

description of the nature of the complex in solution. In the room-temperature ^{1}H NMR of compound **4**, six signals are observed in the aromatic region, corresponding to the six protons of the napy ligand. The most deshielded signal, appearing at 10.21 ppm, is the only one that shows shoulders due to poorly resolved satellites to the NMR active ^{195}Pt nucleus, and it is therefore assigned to the *ortho*-H of the ring coordinated to the platinum center. The presence of six aromatic signals and only one of them exhibiting ^{195}Pt satellites is indicative of the chemical inequivalence of all hydrogen atoms of the napy ligand, as expected due to the coordination to two different metal centers. At the same time, this shows the equivalence of both napy ligands in solution, which is due to the plane of symmetry containing the Pt—Ag bond. Interestingly, the signal corresponding to the *ortho*-H of the ring coordinated to the silver(I) center, appearing at 9.50 ppm, does not show the typical coupling expected due to the close presence to the NMR-active isotopes ^{107}Ag and ^{109}Ag.

The room-temperature ^{19}F NMR spectrum of **4** displays three signals corresponding to the *ortho*- *meta*- and *para*-F of the pentafluorophenyl ligands, indicating that both are chemically equivalent in solution. Noteworthily, the signal corresponding to the *ortho*-F is very broad and not resolved, a characteristic that exists for the resonance of the *meta*-F as well, yet not in such a prominent way. This broadening of the signals can be explained by a rotation process of the C_6F_5 groups about the Pt—C bonds, the broadness of the signals indicating a position close to coalescence. In fact, when measuring the spectrum at 213 K, the rotation process of the pentafluorophenyl groups can be stopped with respect to the NMR time scale, the two *ortho*-F of the rings becoming chemically inequivalent and appearing as two different signals at −116.07 and −120.64 ppm, flanked by ^{195}Pt satellites with coupling constants of $^3J_{F\text{-}Pt} = 575$ Hz and $^3J_{F\text{-}Pt} = 435$ Hz, respectively (Figure 4c). Interestingly, the most deshielded signal shows a more complex multiplicity, which can be tentatively assigned to the through-space coupling to ^{107}Ag and ^{109}Ag in the case of the *ortho*-F that is located closed to the silver(I) center, as it has been detected and described for related systems.[52] By increasing the temperature to 323 K, both signals collapse into one at −118.58 ppm that, despite the fact that it does not show a resolved multiplicity, exhibits ^{195}Pt satellites with $^3J_{F\text{-}Pt} = 528$ Hz (Figure 4c).

A similar reaction was carried out using [Cu(NCMe)$_4$][PF_6] as the source of the acidic copper(I) ion in CH_2Cl_2 aiming at the formation of a Pt—Cu bond. In this case, the Pt(II)−Cu(I) complex *cis*-[Pt(C_6F_5)$_2$(μ-napy)$_2$Cu(NCMe)][PF_6] (**5**, **Figure 5**) was obtained as a deep orange solid in high yield (90%). Nevertheless, contrary to the case of the Pt(II)−Ag(I) complex **4**, the Pt(II)−Cu(I) complex is cationic and bears [PF_6]$^-$ as the counterion. The determination of the molecular structure in the solid state of complex **5** enabled the confirmation of the binuclear character of the complex cation where the two metal centers are bridged by the two napy ligands in *cis* disposition (Figure 5), similar to complex **4** (see Figure 4b), showing yet another example of the retention of the stereochemistry of the starting complex **1**. This points to a close structural similarity of complexes **4** and **5**, considering of course their different neutral/cationic nature. The complex cation in **5** showcases one of the uncommon Pt → Cu donor–acceptor bonds reported thus far,[26,33,34,40–42] with a bond length of 267.16(11) pm. The distance between the metal centers is shorter than those found in Pt(II)−Cu(I) complexes with bridging diphosphine and alkynyl

Journal of Inorganic and General Chemistry
ZAAC
Zeitschrift für anorganische und allgemeine Chemie

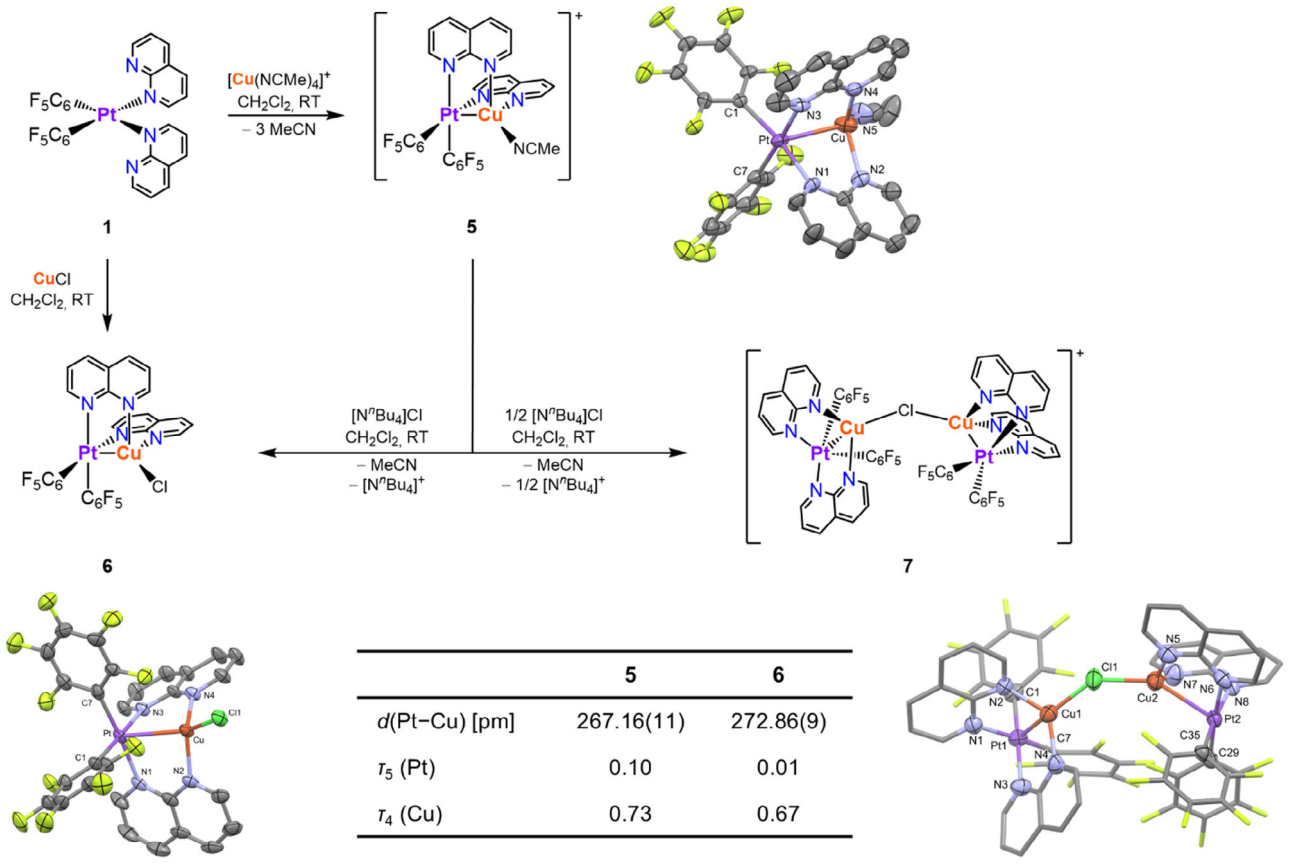

	5	6
d(Pt–Cu) [pm]	267.16(11)	272.86(9)
τ_5 (Pt)	0.10	0.01
τ_4 (Cu)	0.73	0.67

Figure 5. Synthesis of the Pt(II)–Cu(I) complex **5** and exchange reactions with chloride to yield complexes **6** and **7**. In all cases, the anion is $[PF_6]^-$. The molecular structures of *cis*-$[Pt(C_6F_5)_2(\mu\text{-napy})_2Cu(NCMe)]^+$ and *cis*-$[Pt(C_6F_5)_2(\mu\text{-napy})_2CuCl]$ in the solid state are shown, as found in crystals of **5** and **6**, respectively. Hydrogen atoms of napy ligands and the $[PF_6]^-$ anion have been omitted for clarity. Displacement ellipsoids are set at 50% probability. A schematic representation of the $[\{Pt(C_6F_5)_2(\mu\text{-napy})_2Cu\}_2(\mu\text{-Cl})]^+$ anion in the solid state as found in crystals of **7** is also shown, with the first coordination sphere of the metal centers highlighted. Selected bond lengths [pm] and angles [°] for complex **5**: Pt–Cu 267.16(11), Pt–C1 208.(2), Pt–C7 202.2(6), Pt–N1 210.4(5), Pt–N3 210.0(5), Cu–N2 203.6(6), Cu–N4 200.8(6), Cu–N5 194.9(7), C1–Pt–Cu 110.7(5), C1–Pt–N1 167.8(6), C7–Pt–Cu 102.4(2), N1–Pt–Cu 81.34(15), N3–Pt–Cu 83.77(17), C1–Pt–C7 89.6(5), C1–Pt–N3 89.5(5), C7–Pt–N1 89.7(2), C7–Pt–N3 173.7(3), N3–Pt–N1 89.9(2), N4–Cu–N2 113.3(2), N4–Cu–N5 123.8(3), N2–Cu–N5 108.0(3), N4–Cu–Pt 86.1(2), N2–Cu–Pt 86.08(17), N5–Cu–Pt 133.8(2). Selected bond lengths [pm] and angles [°] for complex **6**: Pt–Cu 272.86(9), Pt–C1 201.2(7), Pt–C31 201.1(8), Pt–N1 210.4(7), Pt–N3 210.1(6), Cu–N2 198.4(6), Cu–N4 201.2(6), Cu–Cl1 226.34(19), C1–Pt–Cu 102.5(2), C1–Pt–N1 89.4(3), C31–Pt–Cu 102.01(19), N1–Pt–Cu 82.77(16), N3–Pt–Cu 81.78(15), C1–Pt–C31 88.8(3), C1–Pt–N3 175.5(2), C31–Pt–N1 175.2(2), C31–Pt–N3 91.9(3), N3–Pt–N1 89.6(2), N4–Cu–N2 119.7(3), N4–Cu–Cl1 111.11(17), N2–Cu–Cl1 110.66(19), N4–Cu–Pt 84.70(16), N2–Cu–Pt 84.83(18), Pt–Cu–Cl1 145.25(7). For crystallographic details see the Supporting Information.

ligands,[33,34] yet not as short as in the neutral unsupported complex [(NN)PtMe$_2$]CuOTf (239.92(16) pm, NN = α-diimine ligand)[42] or in cationic complexes with a bridging methyl ligand (252.75 pm),[41] or containing also ligands with the napy scaffold (262.85(3) pm av.), able to bring metal centers in close proximity.[40]

The platinum(II) center exhibits a distorted square-pyramidal five-coordinated environment ($\tau_5 = 0.10$),[48] in which the copper(I) atom occupies the apical position of the pyramid. The coordination environment of the Cu(I) center can be described as a distorted tetrahedron ($\tau_4 = 0.73$),[45] formed by one nitrogen atom of each napy ligand, the platinum center and the nitrogen atom of the acetonitrile ligand that remains coordinated. Interestingly, the three Cu—N distances are identical within the experimental error, even if the nitrogen atoms belong to different types of ligands. The Pt—Cu line is practically perpendicular to the basal plane of the square pyramid containing the platinum(II) center, with an angle between the Pt–Cu axis and the vector perpendicular to the best coordination plane of the platinum center of 13(1)°.

The nature of complex **5** was further confirmed by NMR spectroscopy. In fact, both the ^{1}H and the ^{19}F NMR spectra are quite similar to those of **4**. In the ^{1}H NMR spectrum at room temperature, the six signals for the napy ligands, with only one flanked by ^{195}Pt satellites, account for the equivalence of the napy ligands within the complex and the inequivalence of the two fused pyridine rings, in accordance with the coordination to two different metal centers. Interestingly, the signals corresponding to the ring coordinated to the copper center appear at lower field in comparison to the corresponding signals of complex **4**, which incorporates a silver center. Additionally, the signal at 2.19 ppm confirms the coordination of one molecule of acetonitrile to

the copper center. In the room-temperature ^{19}F NMR spectrum of **5**, a broad signal at −118.08 ppm corresponding to the *ortho*-F of the two equivalent C_6F_5 ligands (Figure S30, Supporting Information) is indicative of a similar coalescence phenomenon as that already described for **4**. In fact, when lowering the temperature to 213 K, two signals appear clearly differentiated (Figure S34, Supporting Information), proving the chemical inequivalence of both *ortho*-F of the same ring since the rotation about the Pt—C bond is stopped. The most deshielded one exhibits a very broad shape and the one that appears at higher field displays satellites with $^3J_{F\text{-}Pt} = 420$ Hz. This comes together with a broadening of the signal for the *meta*-F atoms, pointing also towards a similar coalescence phenomenon. As it has been described for complex **4**, recording the spectra at 323 K leads to the coalescence of the two *ortho*-F signals into one (Figure S34, Supporting Information), therefore indicating the free rotation about the Pt—C bond.

The remaining acetonitrile ligand coordinated to the copper center in **5** can be readily displaced by chloride, leading to the neutral complex *cis*-[Pt(C_6F_5)$_2$(μ-napy)$_2$CuCl] (**6**, Figure 5). A more direct approach starting from **1** and CuCl also allows the synthesis of **6** in CH_2Cl_2 in a similar yield (ca. 70%). NMR spectroscopic data provide hints into the structural nature of complex **6** being similar to that of **5**, the two napy ligands being equivalent in both cases, as well as the two C_6F_5 groups adopting a *cis* configuration. This fact is further proved by IR spectroscopy, since in both cases two bands for the X-sensitive mode of the C_6F_5 groups appear at 798 and 809 cm^{-1} (for **5**) and at 801 and 809 cm^{-1} (for **6**), complemented by ν(C—F) vibrations at 957 and 962 cm^{-1}, respectively, indicating the coordination to a Pt(II) center. Additionally, structural characterization of **6** by means of X-ray diffraction showcases a main difference with the complex cation in **5**: the Pt(II)—Cu(I) bond is elongated to 272.86(9) pm. The platinum(II) center shows an even less distorted square-pyramidal five-coordinate environment ($\tau_5 = 0.01$),[48] whereas the copper(I) is a more distorted tetrahedron ($\tau_4 = 0.67$)[45] than in **5**. The Pt—Cu line is similarly perpendicular to the basal plane of the square pyramid containing the platinum(II) center, with a very similar angle between the Pt—Cu axis and the vector perpendicular to the best coordination plane of the platinum center of 13.9(10)°. The larger distortion respect to the coordination environment found in complex **5** can be a consequence of the weaker Pt → Cu donor–acceptor bond that is compensated by a stronger Cu—Cl bond (226.34(19) ppm), which is shorter than the mean found for Cu(I)—Cl(terminal) distances where the coordination index is four.[53]

Interestingly, when the reaction between **5** and [N^{n}Bu$_4$]Cl is performed in a 2:1 ratio, cluster [{Pt(C_6F_5)$_2$(μ-napy)$_2$Cu}$_2$(μ-Cl)][PF_6] (**7**) is obtained as a brown powder. A preliminary analysis by IR spectroscopy already demonstrated the presence of two C_6F_5 in *cis* arrangement (X-sensitive bands at 795 and 812 cm^{-1}) coordinated to a Pt(II) center (ν(C—F) at 962 cm^{-1}), yet no assumption about the nuclearity of the species could be made. In this case, the determination of the molecular structure in the solid state by X-ray diffraction was crucial to confirm the tetranuclear character of the cation of complex **7**. Unfortunately, the quality of the crystallographic data did not permit a complete resolution of the structure, yet the connectivity of **7** could be fully and unambiguously established. The cation in complex **7** is formed by two heterobinuclear units connected by a chlorido ligand bridging both copper atoms (Figure 5). Each binuclear unit contains a Pt → Cu donor–acceptor bond that is supported by two napy ligands, in which each platinum center is five-coordinated and each copper center is four-coordinated. In the ^1H NMR spectrum of complex **7**, six broad aromatic signals appear (Figure S39, Supporting Information), which get resolved upon lowering the temperature to 193 K (Figure S41, Supporting Information). This indicates the chemical equivalence of the four napy ligands and inequivalence of both pyridine rings within the ligand, similarly to the case of complexes **5** and **6**, and as expected due to the coordination of the napy ligands to two different metal centers. Nevertheless, the coupling constant $^3J_{F\text{-}Pt}$ is too small to be determined. By its side, the ^{19}F NMR spectrum shows again the broad and poorly resolved signal for the *ortho*-F (Figure S40, Supporting Information), related to the rotation process about the Pt—C bonds previously described for complexes **5** and **6**, which is also split into two different signals when the spectrum is measured at 193 K (Figure S42, Supporting Information) due to the free rotation about the Pt—C bond being stopped.

3. Conclusions

Mononuclear platinum complexes *cis*-[Pt(C_6F_5)$_2$(napy)$_2$] (**1**) and *cis*-[Pt(C_6F_5)Cl(napy)$_2$] (**3**) containing two napy ligands coordinated in a monodentate fashion were synthesized by different routes. Compound **1** proved to be a suitable precursor for the synthesis of heterobimetallic donor–acceptor complexes of the type Pt → M (M = Ag, Cu). The uncoordinated nitrogen atoms of the napy ligands of complex **1** are located on either side of the platinum molecular plane. However, the reaction with acidic metal ions to yield complexes *cis*-[Pt(C_6F_5)$_2$(μ-napy)$_2$Ag($OClO_3$)] (**4**) and *cis*-[Pt(C_6F_5)$_2$(μ-napy)$_2$Cu(NCMe)][PF_6] (**5**) causes a change of the initial arrangement to place them on the same side, with each napy ligand bridging the two metal atoms. Furthermore, the symmetric behavior of the pentafluorophenyl groups of complex **1** in solution at room temperature can be explained by the free rotation of both C_6F_5 groups about the Pt—C bonds, but also by the free rotation of the napy ligands despite their larger volumes. However, the NMR equivalence of the pentafluorophenyl groups in binuclear complexes **4** and **5** with the napy ligands bridging the Pt—M bonds (M = Ag, Cu) can only be due to rotation about the Pt—C bonds.

Complex cation **5** entails one more example of the few Pt → Cu donor–acceptor bonds reported thus far showing a short Pt—Cu bond. The uniqueness of this compound was used to explore its reactivity towards the substitution of the acetonitrile ligand by chloride, therefore allowing the synthesis of complexes *cis*-[Pt(C_6F_5)$_2$(μ-napy)$_2$CuCl] (**6**) and [{Pt(C_6F_5)$_2$(μ-napy)$_2$Cu}$_2$(μ-Cl)][PF_6] (**7**). A comparison of the structures of complexes **5** and **6** revealed that the Pt—Cu bond length depends on the auxiliar ligand coordinated to the copper atom (MeCN vs. Cl).

4. Experimental Section

General Procedures and Materials: Unless otherwise indicated, the reactions and manipulations were carried out under ambient conditions at room temperature. Compounds $[N^nBu_4]_2[Pt(C_6F_5)_4]$,[54] $[NBu_4]_2[Pt_2(C_6F_5)_4(\mu\text{-}Cl)_2]$,[55] and *cis*-$[Pt(C_6F_5)_2(thf)_2]$[56] were prepared as reported in the literature. All other reagents were purchased from standard commercial suppliers and used as received. Elemental analyses were carried out using a PerkinElmer 2400 CHNS/O Series II microanalyzer. IR spectra were recorded on neat solid samples using a PerkinElmer Spectrum FT-IR spectrometer (4000–250 cm^{-1}) equipped with an ATR device. Alternatively, some IR spectra were measured using Nujol mulls between polyethylene sheets. NMR spectra were recorded on Bruker ARX 300, Bruker AV 400, or Varian Unity 300 spectrometers. Unless otherwise stated, the spectroscopic measurements were carried out at room temperature. All reported chemical shifts (δ in ppm) are given with respect to the standard references in use: $SiMe_4$ (^1H) and $CFCl_3$ (^{19}F). Where applicable, resonances were assigned by means of ^1H-^1H COSY experiments. The numbering scheme for the assignments of the signals corresponding to the 1,8-naphthyridine ligand in the prepared complexes is given in **Figure 6**. Multiplicity is indicated as follows: s = singlet, d = doublet, m = multiplet, dd = doublet of doublets, tt = triplet of triplets, br = broad, and sh = shouldered.

Synthesis of *cis*-$[Pt(C_6F_5)_2(napy)_2]$ (1): ***Method A***: Two equivalents of the napy ligand (116 mg, 0.891 mmol) were added to a solution of *cis*-$[Pt(C_6F_5)_2(thf)_2]$ (300 mg, 0.445 mmol) in CH_2Cl_2 (30 mL). After 30 min of stirring at room temperature, all volatiles were removed under vacuum. Addition of 20 mL $CHCl_3$ to the residue afforded a yellow solid that was filtered, dried under vacuum and identified as compound **1** (280 mg, 0.355 mmol, 80% yield). ***Method B***: An excess of the napy ligand (145 mg, 1.12 mmol) was added to a solution of $[N^nBu_4]_2[Pt_2(C_6F_5)_4(\mu\text{-}Cl)_2]$ (300 mg, 0.186 mmol) in $CHCl_3$ (15 mL) and the reaction mixture refluxed for 5 h. The formed yellow solid was filtered, washed with ^{i}PrOH (2 × 2 mL) and *n*-hexane (2 × 3 mL), dried under vacuum, and identified as compound **1** (61.0 mg, 77.3 µmol, 83%). ***Method C***: To a solution of $[N^nBu_4]_2[Pt(C_6F_5)_4]$ (200 mg, 0.148 mmol) in MeOH (10 mL), an excess of the napy ligand (193 mg, 1.48 mmol) and two equivalents of $HClO_4$ (1.70 mL, 0.297 mmol, 0.175 M in MeOH) were added. After stirring for a few minutes at room temperature, the colorless solution turned yellow and a solid started to precipitate. After 45 min of stirring, the yellow solid was filtered, washed with ^{i}PrOH (2 × 2 mL) and *n*-hexane (2 × 3 mL), dried under vacuum and identified as compound **1** (88.0 mg, 0.111 mmol, 75%). **^{1}H NMR** (400.13 MHz, $(CD_3)_2CO$, 298 K; Figure S1, Supporting Information): δ_H/ppm = 9.87 (dd, 2H, $^3J_{H1\text{-}H2}$ = 5.18 Hz, $^4J_{H1\text{-}H3}$ = 1.46 Hz, sh, H_1), 9.15 (dd, 2H, $^3J_{H6\text{-}H5}$ = 4.23 Hz, $^4J_{H6\text{-}H4}$ = 1.78 Hz, H_6), 8.52 (dd, 2H, $^3J_{H3\text{-}H2}$ = 8.19 Hz, $^4J_{H3\text{-}H1}$ = 1.57 Hz, H_3), 8.39 (dd, 2H, $^3J_{H4\text{-}H5}$ = 8.16 Hz, H_4), 7.66 (dd, 2H, H_2), 7.61 (dd, 2H, H_5). **^{19}F NMR** (376.50 MHz, $(CD_3)_2CO$, 298 K; Figure S3, Supporting Information): δ_F/ppm = −120.15 (d, 4F, $^3J_{Fo\text{-}Fm}$ = 24.54 Hz, $^3J_{Fo-195Pt}$ = 486.98 Hz, F_o), −167.85 (t, 2F, $^3J_{Fp\text{-}Fm}$ = 19.54 Hz, F_p), −168.18 (m, 4F, F_m). **^{19}F NMR** (282.40 MHz, CD_2Cl_2, 298 K; Figure S8, Supporting Information): δ_F/ppm = −119.93 (m, 4F, $^3J_{Fo-195Pt}$ = 485.43 Hz, F_o), −164.96 (t, 2F, $^3J_{Fp\text{-}Fm}$ = 19.95 Hz, F_p), −166.61 (m, 4F, F_m). **^{19}F NMR** (282.40 MHz, CD_2Cl_2, 183 K; Figure S12, Supporting Information): δ_F/ppm = −119.66 (m, 2F, F_{o1}), −120.61 (m, 2F, F_{o2}), −163.98 (m, 2F, F_p), −165.53 (m, 4F, F_m). **IR** (ATR, 298 K; Figure S43, Supporting Information): $\tilde{V}/cm^{-1}$ = C_6F_5 (952 (s), 798 (s), 749 (m)), napy (1599 (m), 1572 (w), 1558 (w), 833 (m), 808 (m)). **Elemental analysis** calcd (%) for $PtF_{10}N_4C_{28}H_{12}$: C 42.60, H 1.53, N 7.10; found: C 42.90, H 1.41, N 7.00. Yellow single crystals for X-ray diffraction analysis were obtained by slow diffusion of a layer of *n*-hexane (15 mL) into a solution of compound **1** (ca. 40 mg) in acetone (3 mL) at 243 K.

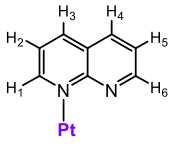

Figure 6. Numbering scheme for the NMR spectroscopic description of the 1,8-naphthyridine ligand in the prepared complexes.

Synthesis of *cis*-$[Pt(C_6F_5)_2Cl(napyH)]$ (2): HCl (2.0 mL, 0.507 mmol, 0.25 M in MeOH) was added to a suspension of **1** (200 mg, 0.253 mmol) in $CHCl_3$ (20 mL). After stirring the yellow suspension for 1.5 h at room temperature, the new yellow solid obtained was filtered, washed first with 10 mL $CHCl_3$ and then with 1 mL Et_2O, dried under vacuum, and identified as **2** (130 mg, 0.187 mmol, 74% yield). Characterization data match those previously reported in the literature.[6]

Synthesis of *cis*-$[Pt(C_6F_5)Cl(napy)_2]$ (3): HCl (0.55 mL, 0.138 mmol, 0.25 M in MeOH) was added to a suspension of **1** (100 mg, 0.127 mmol) in $CHCl_3$ (10 mL). After stirring for 1 h at room temperature, the yellow suspension became a red solution, which eventually turned into an orange suspension. This suspension was then refluxed for 1 h, the color of the suspension turning bright yellow. The obtained yellow solid was filtered, washed first with 2 mL $CHCl_3$ and then with 5 mL *n*-hexane, dried under vacuum, and identified as **3** (39.2 mg, 59.6 µmol, 47% yield). **^{1}H NMR** (400.13 MHz, $(CD_3)_2CO$, 298 K; Figure S16, Supporting Information): δ_H/ppm = 10.09 (dd, 1H, $^3J_{H1\text{-}H2}$ = 5.34 Hz, $^4J_{H1\text{-}H3}$ = 1.76 Hz, H_1), 10.03 (dd, 1H, $^3J_{H1'\text{-}H2'}$ = 5.16 Hz, $^4J_{H1'\text{-}H3'}$ = 1.86 Hz, sh, H_1'), 9.16 (dd, 1H, $^3J_{H6\text{-}H5}$ = 4.24 Hz, $^4J_{H6\text{-}H4}$ = 1.92 Hz, H_6), 9.08 (dd, 1H, $^3J_{H6'\text{-}H5'}$ = 4.23 Hz, $^4J_{H6'\text{-}H4'}$ = 1.94 Hz, H_6'), 8.56 (dd, 1H, $^3J_{H3'\text{-}H2'}$ = 8.20 Hz, H_3'), 8.49 (dd, 1H, $^3J_{H3\text{-}H2}$ = 8.24 Hz, H_3), 8.41 (dd, 1H, $^3J_{H4'\text{-}H5'}$ = 8.26 Hz, H_4'), 8.35 (dd, 1H, $^3J_{H4\text{-}H5}$ = 8.22 Hz, H_4), 7.79 (dd, 1H, H_2'), 7.60 (m, 3H, H_2+H_5+H_5'). **^{19}F NMR** (376.50 MHz, $(CD_3)_2CO$, 298 K; Figure S18, Supporting Information): δ_F/ppm = −121.91 (br, 4F, F_o), −167.48 (tt, 2F, $^3J_{Fp\text{-}Fm}$ = 19.51 Hz, $^4J_{Fp\text{-}Fo}$ = 2.17 Hz, F_p), −169.34 (m, 4F, F_m). **IR** (ATR, 298 K; Figure S44, Supporting Information): $\tilde{V}/cm^{-1}$ = C_6F_5 (953 (s), 805 (s)), napy (1601 (w), 1564 (w), 1497 (m), 842 (w), 832 (w), 799 (s)), Cl (346 (m)). **Elemental analysis** calcd (%) for $C_{22}H_{12}ClF_5N_4Pt$: C 40.16, H 1.84, N 8.52; found: C 40.70, H 1.95, N 8.98. Orange single crystals for X-ray diffraction analysis were obtained by slow diffusion of a layer of *n*-hexane (15 mL) into a solution of compound **3** (ca. 30 mg) in acetone (3 mL) at 277 K.

Synthesis of *cis*-$[Pt(C_6F_5)_2(\mu\text{-}napy)_2Ag(OClO_3)]$ (4): $AgClO_4$ (46.0 mg, 0.222 mmol) was added to a stirred solution of **1** (175 mg, 0.222 mmol) in THF (10 mL) in the dark. The yellow solution faded and after a few minutes a solid precipitate started to appear. After 15 min of stirring, the yellow solid was filtered, washed with *n*-hexane (2 × 3 mL), dried under vacuum, and identified as compound **4** (206 mg, 0.207 mmol, 93% yield). **^{1}H NMR** (300.13 MHz, $(CD_3)_2CO$, 298 K; Figure S20, Supporting Information): δ_H/ppm = 10.21 (d, 2H, $^3J_{H1\text{-}H2}$ = 5.22 Hz, sh, H_1), 9.50 (dd, 2H, $^3J_{H6\text{-}H5}$ = 4.60 Hz, $^4J_{H6\text{-}H4}$ = 1.84 Hz, H_6), 8.93 (dd, 2H, $^3J_{H3\text{-}H2}$ = 8.21 Hz, $^4J_{H3\text{-}H1}$ = 1.63 Hz, H_3), 8.84 (dd, 2H, $^3J_{H4\text{-}H5}$ = 8.22 Hz, H_4), 8.03 (dd, 2H, H_2), 7.96 (dd, 2H, H_5). **^{19}F NMR** (282.40 MHz, $(CD_3)_2CO$, 298 K; Figure S23, Supporting Information): δ_F/ppm = −118.50 (br, 4F, F_o), −163.78 (t, 2F, $^3J_{Fp\text{-}Fm}$ = 19.54 Hz, F_p), −165.99 (m, br, 4F, F_m). **^{19}F NMR** (282.40 MHz, $(CD_3)_2CO$, 213 K; Figure S25, Supporting Information): δ_F/ppm = −116.07 (m, 2F, $^3J_{Fo-195Pt}$ = 575.05 Hz, F_{o1}), −120.64 (m, 2F, $^3J_{Fo-195Pt}$ = 434.75 Hz, F_{o2}), −163.19 (t, 2F, $^3J_{Fp\text{-}Fm}$ = 20.14 Hz, F_p), −165.41 (m, 4F, F_m). **IR** (ATR, 298 K, Figure S45, Supporting Information): $\tilde{V}/cm^{-1}$ = C_6F_5 (957 (s), 811 (m), 798 (s)), $[ClO_4]^-$ (1099 (m), 622 (m)), napy (1635 (w), 1606 (w), 1570 (w), 777 (w)). **Elemental analysis** calcd (%) for $C_{28}H_{12}AgClF_{10}N_4O_4Pt$: C 33.74, H 1.21, N 5.62; found: C 33.58, H 1.13, N 5.40. Yellow single crystals for X-ray diffraction analysis were obtained by slow diffusion of a layer of *n*-hexane (15 mL) into a solution of compound **4** (ca. 30 mg) in acetone (3 mL) at 243 K.

Synthesis of *cis*-[Pt(C_6F_5)$_2$(μ-napy)$_2$Cu(NCMe)][PF_6] (5): [Cu(NCMe)$_4$][PF_6] (23.6 mg, 63.3 µmol) was added to a solution of **1** (50.0 mg, 63.3 µmol) in CH_2Cl_2 (5 mL) and stirred at room temperature for 5 min, with a color change of yellow to orange. Et_2O was then added and an orange solid precipitated. The solid was filtered, washed with Et_2O (2 × 3 mL), dried under vacuum and identified as compound **5** (59.4 mg, 57.2 µmol, 90% yield). **^{1}H NMR** (300.13 MHz, $(CD_3)_2CO$, 298 K; Figure S27, Supporting Information): δ_H/ppm = 10.24 (d, 2H, $^3J_{H1\text{-}H2}$ = 5.17 Hz, sh, H_1), 9.63 (dd, 2H, $^3J_{H6\text{-}H5}$ = 4.85 Hz, $^4J_{H6\text{-}H4}$ = 1.78 Hz, H_6), 8.92 (dd, 2H, $^3J_{H3\text{-}H1}$ = 1.68 Hz, H_3), 8.89 (dd, 2H, H_4), 8.06 (dd, 2H, $^3J_{H2\text{-}H3}$ = 8.24 Hz, H_2), 8.00 (dd, 2H, $^3J_{H5\text{-}H4}$ = 8.21 Hz, H_5), 2.19 (s, 3H, NCCH_3). **^{19}F NMR** (282.40 MHz, $(CD_3)_2CO$, 298 K; Figure S30, Supporting Information): δ_F/ppm = −72.66 (d, 6F, $^1J_{F\text{-}P}$ = 707.3 Hz, [PF_6]$^-$), −118.08 (br, 4F, F_o), −163.97 (t, 2F, $^3J_{Fp\text{-}Fm}$ = 19.52 Hz, F_p), −166.31 (m, 4F, F_m). **^{19}F NMR** (282.40 MHz, $(CD_3)_2CO$, 213 K; Figure S32, Supporting Information): δ_F/ppm = −71.88 (d, 6F, $^1J_{F\text{-}P}$ = 708.4 Hz, [PF_6]$^-$), −114.65 (br, 2F, F_{o1}), −120.52 (m, 2F, $^3J_{Fo-195Pt}$ = 420.24 Hz, F_{o2}), −163.35 (t, 2F, $^3J_{Fp\text{-}Fm}$ = 20.08 Hz, F_p), −165.67 (m, 4F, F_m). **IR** (ATR, 298 K; Figure S46, Supporting Information): $\tilde{V}$/cm^{-1} = C_6F_5 (957 (m), 809 (m), 798 (m)), [PF_6]$^-$ (848 (m), 557 (m)), napy (1635 (m), 1606 (w), 1572 (w), 837 (w), 832 (w)), $NCCH_3$ (2165 (w)). **Elemental analysis** calcd (%) for: $C_{30}H_{15}CuF_{16}N_5PPt$: C, 34.68; H, 1.46; N, 6.74; found: C, 34.31; H, 1.21; N, 5.95. Single crystals for X-ray diffraction analysis were obtained by slow diffusion of a layer of *n*-hexane (15 mL) into a solution of compound **5** (ca. 30 mg) in 1,2 dichloroethane (3 mL) at 277 K.

Synthesis of *cis*-[Pt(C_6F_5)$_2$(μ-napy)$_2$CuCl] (6): ***Method A*:** [N^{n}Bu$_4$]Cl·H_2O (57.0 mg, 0.192 mmol) was added to a solution of **5** (200 mg, 0.192 mmol) in CH_2Cl_2 (30 mL). The orange solution turned immediately brown and a solid started to precipitate. After stirring for 10 min at room temperature the brown solid was filtered, washed with 5 mL CH_2Cl_2, dried under vacuum, and identified as **6** (120 mg, 0.135 mmol, 70% yield). ***Method B*:** CuCl (18.8 mg, 0.190 mmol) was added to a solution of **1** (150 mg, 0.190 mmol) in CH_2Cl_2 (30 mL) The yellow solution turned immediately brown and a solid started to precipitate. After stirring for 10 min at room temperature, the brown solid was filtered, washed with 5 mL *n*-hexane, dried under vacuum, and identified as **6** (121 mg, 0.136 mmol, 72% yield). **^{1}H NMR** (300.13 MHz, $(CD_3)_2CO$, 193 K; Figure S37, Supporting Information): δ_H/ppm = 10.28 (br, 2H, H_1), 9.90 (br, 2H, H_6), 8.90 (br, 2H, $H_3 + H_4$), 8.06 (br, 2H, H_2), 7.94 (br, 2H, H_5). **^{19}F NMR** (282.40 MHz, $(CD_3)_2CO$, 193 K; Figure S38, Supporting Information): δ_F/ppm = −110.07 (m, 2F, $^3J_{Fo-195Pt}$ = 494.20 Hz, F_{o1}), −119.42 (m, 2F, $^3J_{Fo-195Pt}$ = 451.80 Hz, F_{o2}), −162.90 (m, 2F, F_p), −164.71 (m, 2F, F_{m1}), −165.30 (m, 2F, F_{m2}). **IR** (ATR, 298 K; Figure S47, Supporting Information): $\tilde{V}$/cm^{-1} = C_6F_5 (962 (s), 809 (s), 801 (s)), napy (1569 (m), 837 (m), 437 (w)). **Elemental analysis** calcd (%) for $C_{28}H_{12}ClCuF_{10}N_4Pt{\cdot}CH_2Cl_2$: C 35.78, H 1.45, N 5.76; found: C 35.73, H 1.49, N 5.60. Single crystals for X-ray diffraction analysis were obtained by slow diffusion of a layer of *n*-hexane (15 mL) into a solution of compound **6** (ca. 40 mg) in 1,2-dichloroethane (3 mL) at 277 K.

Synthesis of [{Pt(C_6F_5)$_2$(μ-napy)$_2$Cu}$_2$(μ-Cl)][PF_6] (7): [N^{n}Bu$_4$]Cl·H_2O (28.5 mg, 96.2 µmol), was added to a solution of **5** (200 mg, 0.192 mmol) in CH_2Cl_2 (30 mL). The orange solution turned immediately brown. After stirring for 20 min at room temperature, all volatiles were evaporated to dryness. The residue was then treated with 10 mL $CHCl_3$, resulting in a brown solid that was filtered, dried under vacuum, and identified as **7** (304 mg, 0.161 mmol, 84% yield). **^{1}H NMR** (300.13 MHz, $(CD_3)_2CO$, 193 K; Figure S41, Supporting Information): δ_H/ppm = 10.35 (br, 4H, H_1), 10.18 (br, 4H, H_6), 8.97 (d, 4H, $^3J_{H3\text{-}H2}$ = 7.90 Hz, H_3), 8.90 (d, 4H, $^3J_{H4\text{-}H5}$ = 8.10 Hz, H_4), 8.12 (dd, 4H, $^4J_{H2\text{-}H1}$ = 5.10 Hz, H_2), 7.92 (dd, 4H, $^4J_{H5\text{-}H6}$ = 4.90 Hz, H_5). **^{19}F NMR** (282.40 MHz, $(CD_3)_2CO$, 193 K; Figure S42, Supporting Information): δ_F/ppm = −110.20 (m, 4F, $^3J_{Fo-195Pt}$ = 485.40 Hz, F_{o1}), −119.84 (m, 4F, $^3J_{Fo-195Pt}$ = 406.00 Hz, F_{o2}), −163.02 (m, 4F, F_p), −165.17 (m, 4F, F_{m1}), −166.30 (m, 4F, F_{m2}). **IR** (ATR, 298 K; Figure S48, Supporting Information): $\tilde{V}$/cm^{-1} = C_6F_5 (962 (s), 812 (s), 795 (s)), [PF_6]$^-$ (848 (s), 559 (s)), napy (1571 (m), 437 (w)). **Elemental analysis** calcd (%) for $C_{56}H_{24}ClCu_2F_{26}N_8PPt_2$: C 35.65, H 1.28, N 5.94; found: C 34.96, H 1.59, N 5.76. Single crystals were obtained by slow diffusion of a layer of *n*-hexane (15 mL) into a solution of compound **7** (ca. 40 mg) in 1,2-dichloroethane (3 mL) at 277 K.

Crystal Data and X-Ray Structure Determination: Single crystals suitable for X-ray diffraction studies were obtained as indicated in the corresponding experimental entry. Crystal data and other details of the structure analysis are presented in Table S1 in the Supporting Information, together with the details of diffraction data collection and structure solution.

Acknowledgements

This work was supported by the Spanish MICIU/FEDER (Grant PID2021-122869NB-I00 funded by MICIU/AEI/10.13039/501100011033 and ERDF/EU) and the Gobierno de Aragón (Grupo E17_23R: *Química Inorgánica y de los Compuestos Organometálicos*). A.P.-B. thanks the Spanish MECD for a predoctoral grant (FPU15/03940) and the Fonds der Chemischen Industrie for a Liebig Fellowship.

Open Access funding enabled and organized by Projekt DEAL.

Conflict of Interest

The authors declare no conflict of interest.

Data Availability Statement

The data that support the findings of this study are available in the supplementary material of this article.

Keywords: 1,8-naphthyridine · bimetallic complex · metal–metal bond · pentafluorophenyl · platinum

[1] J. K. Bera, N. Sadhukhan, M. Majumdar, *Eur. J. Inorg. Chem.* **2009**, 4023.
[2] M. A. Ciriano, L. A. Oro, in *Comprehensive Coordination Chemistry II*, Vol. *1* (Eds: J. A. M. Cleverty, T. J. Meyer), Elsevier, Amsterdam **2003**, pp. 55–61.
[3] I. Ara, J. M. Casas, J. Forniés, A. J. Rueda, *Inorg. Chem.* **1996**, *35*, 7345.
[4] C. Tubaro, G. Greggio, S. Antonello, C. Graiff, A. Biffis, *Inorg. Chim. Acta* **2017**, *466*, 578.
[5] J. M. Casas, B. E. Diosdado, L. R. Falvello, J. Forniés, A. Martín, A. J. Rueda, *Dalton Trans.* **2004**, 2733.
[6] J. M. Casas, B. E. Diosdado, J. Forniés, A. Martín, A. J. Rueda, A. G. Orpen, *Inorg. Chem.* **2008**, *47*, 8767.
[7] T. Tomon, T.-a. Koizumi, K. Tanaka, *Angew. Chem. Int. Ed.* **2005**, *44*, 2229.
[8] T. Mizukawa, K. Tsuge, H. Nakajima, K. Tanaka, *Angew. Chem. Int. Ed.* **1999**, *38*, 362.
[9] H. Nakajima, K. Tanaka, *Chem. Lett.* **1995**, *24*, 891.
[10] V. K. Jain, L. Jain, *Coord. Chem. Rev.* **2005**, *249*, 3075.
[11] M. Chaaban, C. Zhou, H. Lin, B. Chyi, B. Ma, *J. Mater. Chem. C* **2019**, *7*, 5910.
[12] R. J. Puddephatt, *J. Organomet. Chem.* **2017**, *849-850*, 268.

[13] J. R. Berenguer, E. Lalinde, M. T. Moreno, *Coord. Chem. Rev.* **2018**, *366*, 69.
[14] Á. Díez, E. Lalinde, M. T. Moreno, *Coord. Chem. Rev.* **2011**, *255*, 2426.
[15] J. Bauer, H. Braunschweig, R. D. Dewhurst, *Chem. Rev.* **2012**, *112*, 4329.
[16] M.-E. Moret, *Top. Organomet. Chem.* **2011**, *35*, 157.
[17] J. Forniés, A. Martín, in *Metal Clusters in Chemistry*, Vol. *1* (Eds: P. Braunstein, L. A. Oro, P. R. Raithby), Wiley-VCH, Weinheim **1999**, pp. 417–443.
[18] G. Aullón, S. Alvarez, *Inorg. Chem.* **1996**, *35*, 3137.
[19] C. Mealli, F. Pichierri, L. Randaccio, E. Zangrando, M. Krumm, D. Holtenrich, B. Lippert, *Inorg. Chem.* **1995**, *34*, 3418.
[20] The diversity of Pt(II)−Ag(I) complexes reported before 2018 is covered with great detail in several reviews, where plenty of examples can be found: See Refs. 13, 14, and 17. For selected more recent examples, see references 21, 22, 23, 24, 25 and 26.
[21] J. Roy, M. Forzatti, L. Arnal, A. Martín, S. Fuertes, D. Tordera, V. Sicilia, *Inorg. Chem.* **2024**, *63*, 7275.
[22] N. K. Sinha, V. Mishra, N. Thirupathi, *Inorg. Chem.* **2023**, *62*, 7644.
[23] J. Quan, Z.-H. Chen, X. Zhang, J.-Y. Wang, L.-Y. Zhang, Z.-N. Chen, *Inorg. Chem. Front.* **2021**, *8*, 2323.
[24] D. Campillo, Ú. Belío, A. Martín, *Dalton Trans.* **2019**, *48*, 3270.
[25] M. Baya, Ú. Belio, D. Campillo, I. Fernández, S. Fuertes, A. Martin, *Chem. Eur. J.* **2018**, *24*, 13879.
[26] O. Crespo, M. C. Gimeno, A. Laguna, O. Lehtonen, I. Ospino, P. Pyykkö, M. D. Villacampa, *Chem. Eur. J.* **2014**, *20*, 3120.
[27] L. Kaufmann, S. A. Föhrenbacher, M. C. Krummer, B. Butschke, *Eur. J. Inorg. Chem.* **2024**, *27*, e202300577.
[28] D.-S. Zheng, M. Yang, J.-Y. Wang, Z.-N. Chen, *ACS Appl. Mater. Interfaces* **2022**, *14*, 23669.
[29] H. Zeng, J.-Y. Wang, L.-X. Shi, L.-Y. Zhanga, Z.-N. Chen, *Inorg. Chem. Front.* **2022**, *9*, 3156.
[30] M. Baya, Ú. Belío, I. Fernández, S. Fuertes, A. Martín, *Angew. Chem. Int. Ed.* **2016**, *55*, 6978.
[31] F. Juliá, P. G. Jones, P. González-Herrero, *Inorg. Chem.* **2012**, *51*, 5037.
[32] J. Vicente, P. González-Herrero, M. Pérez-Cadenas, *Inorg. Chem.* **2007**, *46*, 4718.
[33] G.-Q. Yin, Q.-H. Wie, L.-Y. Zhang, Z.-N. Chen, *Organometallics* **2006**, *25*, 580.
[34] B.-H. Xia, H.-X. Zhang, C.-M. Che, K.-H. Leung, D. L. Phillips, N. Zhu, Z.-Y. Zhou, *J. Am. Chem. Soc.* **2003**, *125*, 10362.
[35] J. Vicente, M. T. Chicote, S. Huertas, P. G. Jones, A. K. Fischer, *Inorg. Chem.* **2001**, *40*, 6193.
[36] H.-K. Yip, H.-M. Lin, Y. Wang, C.-M. Che, *J. Chem. Soc., Dalton Trans.* **1993**, 2939.
[37] M. Crespo, J. Sales, X. Solans, *J. Chem. Soc., Dalton Trans.* **1989**, 1089.
[38] G. J. Arsenault, C. M. Anderson, R. J. Puddephatt, *Organometallics* **1988**, *7*, 2094.
[39] A. Albinati, H. Lehner, L. M. Venanzi, M. Wolfer, *Inorg. Chem.* **1987**, *26*, 3933.
[40] S. Deolka, O. Rivada-Wheelaghan, S. L. Aristizábal, R. R. Fayzullin, S. Pal, K. Nozaki, E. Khaskin, J. R. Khusnutdinova, *Chem. Sci.* **2020**, *11*, 5494.
[41] M.-E. Moret, D. Serra, A. Bach, P. Chen, *Angew. Chem. Int. Ed.* **2010**, *49*, 2873.
[42] M.-E. Moret, P. Chen, *J. Am. Chem. Soc.* **2009**, *131*, 5675.
[43] P. Sgarbossa, U. Śliwińska-Hill, M. F. C. Guedes da Silva, B. Bażanów, A. Pawlak, N. Jackulak, D. Poradowski, A. J. L. Pombeiro, P. Smoleński, *Materials* **2019**, *12*, 3907.
[44] R. Usón, J. Forniés, M. Tomás, B. Menjón, *Organometallics* **1986**, *5*, 1581.
[45] L. Yang, D. R. Powell, R. P. Houser, *Dalton Trans.* **2007**, 955.
[46] R. Usón, J. Forniés, *Adv. Organomet. Chem.* **1988**, *28*, 219.
[47] F. Blank, H. Scherer, J. Ruiz, V. Rodríguez, C. Janiak, *Dalton Trans.* **2010**, *39*, 3609.
[48] A. W. Addison, T. N. Rao, J. Reedijk, J. van Rijn, G. C. Verschoor, *J. Chem. Soc., Dalton Trans.* **1984**, 1349.
[49] R. Usón, J. Forniés, M. Tomás, I. Ara, J. M. Casas, A. Martín, *J. Chem. Soc., Dalton Trans.* **1991**, 2253.
[50] R. Usón, J. Forniés, M. Tomás, J. M. Casas, *Angew. Chem. Int. Ed., Eng.* **1989**, *28*, 748.
[51] R. Usón, J. Forniés, M. Tomás, J. M. Casas, F. A. Cotton, L. R. Falvello, R. Llusar, *Organometallics* **1988**, *7*, 2279.
[52] J. M. Casas, J. Forniés, A. Martín, B. Menjón, M. Tomás, *Polyhedron* **1996**, *15*, 3599.
[53] A. G. Orpen, L. Brammer, F. H. Allen, O. Kennard, D. G. Watson, R. Taylor, *J. Chem. Soc., Dalton Trans.* **1989**, S1-S83.
[54] R. Usón, J. Forniés, F. Martínez, M. Tomás, *J. Chem. Soc., Dalton Trans.* **1980**, 888.
[55] R. Usón, J. Forniés, M. Tomás, R. Fandos, *J. Organomet. Chem.* **1984**, *263*, 253.
[56] R. Usón, J. Forniés, M. Tomás, B. Menjón, *Organometallics* **1985**, *4*, 1912.

Manuscript received: July 27, 2025
Revised manuscript received: September 10, 2025
Version of record online: